https://doi.org/10.5194/egusphere-2025-2397
Preprint. Discussion started: 4 June 2025

The contribution of circulation changes to summer temperature trends in the northern hemisphere mid-latitudes: A multi-method quantification

Peter Pfleiderer[1], Anna Merrifield[2], István Dunkl[1], Durand Homer[3], Enora Cariou[4], Julien Cattiaux[4], and Sebastian Sippel[1]

[1]Institute for Meteorology, Leipzig University, Leipzig, Germany
[2]Institute for Atmospheric and Climate Sciences, ETH Zürich, Switzerland
[3]Image Processing Lab, University of Valencia, Spain
[4]Centre National de Recherches Météorologiques, Université de Toulouse, CNRS, Météo-France, Toulouse, France

Correspondence: Peter Pfleiderer (peter.pfleiderer@uni-leipzig.de)

Abstract. The increase in summer temperature and heat extremes is well documented and attributed to anthropogenic climate change. There is, however, still a vivid debate about the influence of atmospheric circulation changes on summer temperatures and heat extremes. Over the northern hemispheric mid-latitudes, considerable regional differences in summer temperatures have been observed. These differences have been linked to atmospheric circulation changes using statistical methods, but it remains challenging to evaluate such methods on multi-decadal time scales. Here, we evaluate different decomposition methods and systematically investigate circulation-induced summer temperature trends. For the evaluation of statistical and machine learning decomposition methods we use climate model simulations without external forcing but with atmospheric circulation nudged towards the circulation of a freely running simulation forced by anthropogenic emissions and land use changes. We train the decomposition methods on the free-running forced simulation and compare its circulation-induced trends to the trends simulated in the nudged circulation simulation. Most decomposition methods show skill in estimating the sign of circulation-induced trends but all methods underestimate the magnitude of these trends. The application of tested decomposition methods confirms that circulation changes have contributed substantially to an increase in summer heat over several mid-latitude regions, including Europe. In this hotspot region, we estimate that up to half of the warming over the period 1979-2023 is due to circulation changes.

1 Introduction

The intensity of heat waves increases globally, causing considerable ecological and societal impacts. It is well understood that in a warming climate heat waves over few days or warm summer seasons intensify and this effect can be robustly attributed to anthropogenic activities (Seneviratne et al., 2021). The main reason for this intensification is of thermodynamic nature: heat extremes occurring in a warmer atmosphere are also warmer. However, heat waves are not only determined by direct thermodynamic changes in a warming climate: Various effects can lead to regional trends in summer heat including changes in atmospheric circulation (Teng et al., 2022; Rousi et al., 2022; Vautard et al., 2023; Singh et al., 2023), or feedbacks due to

https://doi.org/10.5194/egusphere-2025-2397
Preprint. Discussion started: 4 June 2025

land-atmosphere interactions (Seneviratne et al., 2006). As a result, regional trends in summer average temperatures or summer heat extremes differ strongly across the world and even across the northern hemispheric mid-latitude land area.

In the mid-latitudes, large-scale circulation is a crucial driver for heat extremes (Rousi et al., 2022; Röthlisberger and Papritz, 2023) and there is great interest in understanding to what extent atmospheric circulation contributed to individual events (Cattiaux et al., 2010; Sippel et al., 2024; Zeder and Fischer, 2023), trends in heat extremes (Rousi et al., 2022; Singh et al., 2023) or seasonal temperatures (Teng et al., 2022). Forced changes in jet stream position and strength (Dong et al., 2022; Rousi et al., 2022; Woollings et al., 2023; Shaw and Miyawaki, 2024), changes in storm track intensity (Coumou et al., 2015; Chemke and Coumou, 2024) and the resulting changes in weather pattern frequencies (Horton et al., 2015; Hanna et al., 2018; Fabiano et al., 2021) are likely to affect local climate conditions (Pfleiderer et al., 2019). Over the observational record these forced changes are however small compared to internal climate variability (Eyring et al., 2021). Estimating the contribution of atmospheric circulation changes to local temperature trends and quantifying to which extent these changes are due to forced or internal variability is crucial for our understanding of past summer temperature trends (Merrifield et al., 2017; Teng et al., 2022; Vautard et al., 2023) and extreme events (Terray, 2021).

In some regions, the observed trends are falling out of the range of model-simulated expected trends (e.g., Western Europe, (Teng et al., 2022; Rousi et al., 2022; Vautard et al., 2023; Kornhuber et al., 2024)). Potentially, this may indicate that model-simulated low-frequency variability in large-scale atmospheric circulation is too weak, or that a forced change in circulation is missing in the models, notwithstanding the broad uncertainty across models (Shepherd, 2014). The missing low-frequency hypothesis is also difficult to assess because the available observations are rather short. Understanding past circulation changes and their contribution to temperature trends may provide an opportunity to constrain future changes in summer temperature trends, acknowledging that future circulation changes remain a very large source of uncertainty (Topál and Ding, 2023; Fereday et al., 2018).

However, it is not straightforward to identify circulation-induced contributions to temperature trends (Deser et al., 2016). To empirically study circulation contributions to temperature trends one can either use i) statistical or machine learning methods that decompose the observed or simulated temperature trend in its thermodynamically induced and its circulation induced components, often framed as "dynamical adjustment" (Deser et al., 2016; Smoliak et al., 2015; Sippel et al., 2019) or ii) create nudged circulation simulations where the circulation component is fixed and the thermodynamic component is removed (see e.g., (Wehrli et al., 2018)). Both options have their limitations: Nudged circulation experiments are limited by the representation of physical mechanisms in the climate model used. On the other hand, most of statistical decomposition methods are designed to capture the relationship between daily circulation patterns and daily temperatures and they do indeed capture day-to-day variability very well, and good skill is obtained on monthly or inter-annual time scales as well (Smoliak et al., 2015; Sippel et al., 2019; Cariou et al., 2025). Whether they can adequately capture a long-term trend is however more difficult to test, because processes determining long-term trends may be distinctly different from those that determine short-term circulation variability; and much fewer verification samples are available. Moreover, benchmarks for circulation-induced long-term trends have not been available so far, and to our knowledge no systematic comparison of dynamical adjustment methods has been performed.

https://doi.org/10.5194/egusphere-2025-2397
Preprint. Discussion started: 4 June 2025

In this study, we provide a robust overview of circulation induced summer temperature trends over the northern hemispheric mid-latitudes by making use of a combination of statistical decomposition methods and nudged circulation experiments. We address two specific research questions: First, we evaluate whether statistical-empirical methods are able to correctly estimate circulation-induced long-term trends against a climate model benchmark. The climate model benchmark experiment is specifically designed as a set of CESM2 nudged circulation simulations, which allows comparison of circulation-induced trend components against statistical decomposition methods. Second, we identify circulation-induced summer temperature trends across the northern hemispheric mid-latitudes in observations using four different statistical methods; and CESM2 simulations that are nudged to the ERA5 circulation, but that are driven without anthropogenic forcing.

2 Data & Methods

This study is mainly based on simulations of the fully coupled Community Earth System Climate Model, Version 2 (CESM2) (Danabasoglu et al., 2020) including simulations from the CESM2 large ensemble (Rodgers et al., 2021). In section 3.2 we apply decomposition methods to the European Centre for Medium-Range Weather Forecasts (ECMWF) Reanalysis v5 (ERA5) (Hersbach et al., 2020).

2.1 CESM2 nudged circulation simulations driven with CESM2 horizontal winds

To derive a benchmark for the evaluation of the decomposition methods, we use nudged circulation experiments that have been conducted with the fully coupled CESM2 (Danabasoglu et al., 2020). First, three standard historical and future anthropogenic forcing experiments are simulated following historical greenhouse gas emissions, aerosol emissions and land use changes in the period 1850-2014, and anthropogenic forcings following the SSP3-70 scenario from then onwards ('hist+SSP370'). These simulations follow the protocol of the CESM2 large ensemble (Rodgers et al., 2021).

In a second step, for each of these simulations a nudged circulation simulation is created for piControl forcing (e.g. no anthropogenic greenhouse gas and aerosol emissions as well as no land use change). Each of these simulations starts with the same initial conditions as their corresponding hist+ssp370 simulation; 6-hourly global meridional and horizontal winds throughout the atmosphere (all vertical levels) and globally are nudged to their corresponding hist+ssp370 simulation. The nudging is achieved via a regular relaxation procedure described in the CAM6 handbook (camdoc), and is similar to Topál and Ding 2023. These simulations will be henceforth referred to 'piControl-nudged', as they lack the direct anthropogenic forcing but through the nudging of atmospheric circulation any potential anthropogenic forcing on horizontal wind fields are present alongside with the internal circulation variability of the atmosphere from the hist+ssp370 simulation.

2.1.1 Conceptual Interpretation of CESM2 nudged circulation simulations as a benchmark for dynamical adjustment

In a free-running, fully coupled climate simulation, local or regional temperatures are affected both by thermodynamic forcing represented by global mean surface temperature (GMST) as well as atmospheric circulation variability (e.g.; Deser et al.

https://doi.org/10.5194/egusphere-2025-2397
Preprint. Discussion started: 4 June 2025

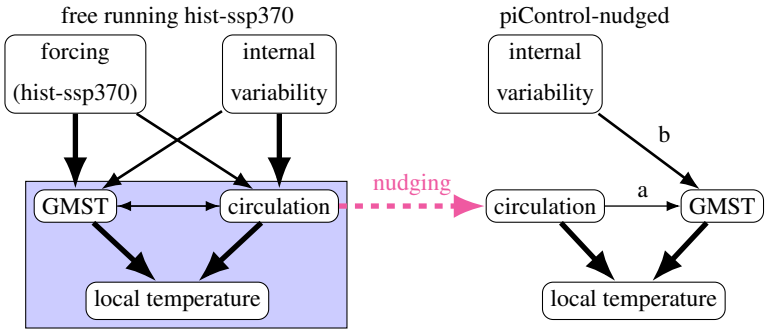

Figure 1. Conceptual illustration of causal relationships influencing local temperatures in a freely running climate simulation (left) and in a piControl-nudged simulation (right). The arrow width indicates assumed importance of links. The blue rectangle highlights the processes studied here.

2016, figure 1), and interactions between both. Statistical dynamical adjustment methods aim to separate those influences, but the skill of those methods is inherently difficult to evaluate in a coupled system. Hence, the goal of our 'piControl-nudged' simulations is to derive benchmark simulations, in which only circulation is changing, while thermodynamic forcing is fixed to pre-industrial values. This will allow to evaluate the circulation contribution independently from the trends in thermodynamic forcing. The conceptual interpretation of the 'piControl-nudged' simulations is sketched in figure 1: Circulation variability is 'inherited' from its parent simulation, which we expect to determine local and regional temperatures to the largest extent. The inherited circulation variability may contain both internal variability from the parent simulation, but also potential forced circulation changes. Moreover, we expect that some internal variability that is independent from atmospheric circulation may remain in the 'piControl-nudged' simulations, for example due to ocean variability that may affect GMST (arrow b in Fig. 1).

2.1.2 Illustration of CESM2 nudged circulation simulations

As expected, day-to-day variability in the nudged circulation run is closely related to its freely running counterpart from which the wind fields originated from. As shown in figure A1 in the early period, geopotential height at 500 hPa and surface air temperature are nearly identical in the hist+ssp370 and the piControl-nudged run. In a warmer climate, the day-to-day variability is still highly correlated, but geopotential height and surface air temperatures are uniformly shifted to higher values. However, interpreting the GMST signal in the piControl-nudged runs is somewhat challenging. Despite the absence of external forcing, small trends in GMST can be found over 40-year periods in the piControl-nudged simulations (compare figure 2b,c). These trends may be driven by atmospheric circulation and internal variability in the ocean dynamics (see figure 1).

A comparison of 1979-2023 GMST trends in the piControl-nudged simulations with their corresponding freely running forced simulations indicates that both of these processes are relevant (figure 2b): The run 1 is the simulation with highest GMST trend in the freely running as well as in the piControl-nudged simulation while run 3 has lowest GMST trends in both simulations. The differences between freely running simulations and their corresponding piControl-nudged simulations are not constant, indicating that there is indeed an influence of internal variability that is not controlled by atmospheric circulation.

https://doi.org/10.5194/egusphere-2025-2397
Preprint. Discussion started: 4 June 2025

Therefore, we do not expect that the circulation component estimated from the freely running forced simulation matches the trend found in the piControl-nudged simulation exactly. However, we assume that the effect of GMST on local temperatures is rather homogeneous around the northern hemispheric mid-latitudes, and thus we expect that the spatial pattern relative to the mid-latitudinal mean is well captured.

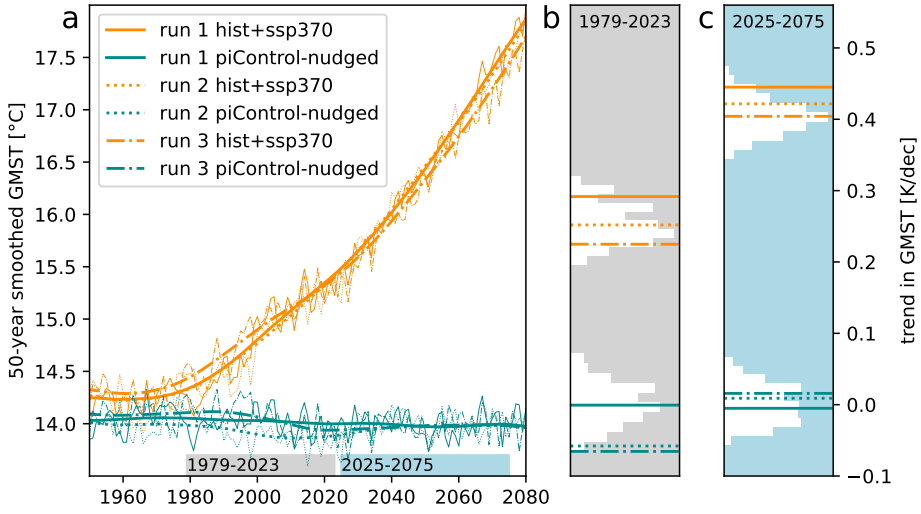

Figure 2. a: Global mean surface temperature in hist+ssp370 runs (orange) and in piControl-nudged runs (green). b: GMT trend over the period 1979-2023 (gray bar in a). c: GMT trend over the period 2025-2075 (blue bar in a). The cooler histogram depicts 500 trends of the same length from piControl, the warmer historgram depicts 100 trends from the CESM2 large ensemble.

2.2 CESM2 nudged circulation simulations driven with ERA5 winds

To evaluate the use of the decomposition methods on observed circulation patterns, we created an additional benchmark simulation by nudging CESM2 to the horizontal wind fields from the reanalysis data ERA5 (Hersbach et al., 2020). This method relies on the same relaxation procedure and anthropogenic forcing as described before, with some modifications to the setup. Here not only the piControl, but also the 'hist+SSP370' simulations are nudged to ERA5 horizontal wind fields between 1940 and 2024. In order to account for forcing-induced variability at the boundary later, the atmosphere is only nudged above 700 hPa, similar to (Wehrli et al., 2018). The model is run in an AMIP setup with a prescribed ocean from the Met Office Hadley Centre's sea ice and sea surface temperature data set (HadISST, Rayner et al. (2003)). To create the sea surface temperature data for the piControl simulation, we removed the forced component from HadISST with a low-frequency pattern filtering (Wills et al., 2020). We estimate piControl Sea Ice Concentration (SIC) by applying a random forest model to the relationship between Sea Surface Temperature (SST) and SIC in the HadISST data. To account for seasonal hysteresis, we train separate models for the freezing (Sept-Jan) and melting (Feb-Aug) seasons, and then apply these models to piControl SSTs to generate match-

https://doi.org/10.5194/egusphere-2025-2397
Preprint. Discussion started: 4 June 2025

ing SIC values. While this approach allows a good reproduction of daily temperature anomalies on the northern hemisphere, nudging to observed winds and SSTs introduces a temperature bias by removing the model from its own climatology.

2.3 Dynamical adjustment methods

We test four methods designed to disentangle the dynamic effect from the thermodynamic effect: (1) ridge regression, (2) constructed circulation analogues, (3) direct effect analysis (DEA), and a neural network UNET (4).

2.3.1 Ridge regression

For each grid-cell, we train a linear regression model to predict daily mean temperatures in summer (June-July-August from here on JJA) (Y) using as covariates GMST (yearly averaged) and the streamfunction (Φ) at 500hPa in grid-cells in a rectangle of 40x40 degree around that grid-cell.

$$Y = \gamma_0 + \gamma_1 GMST + \sum_{j}^{grid-cells} (\gamma_j \Phi_j) + \epsilon \tag{1}$$

The streamfunction (Φ) is related to horizontal eastward (U) and northward (V) wind speeds in the following way:

$$u = \frac{\partial \Phi}{\partial y}, v = \frac{\partial \Phi}{\partial x} \tag{2}$$

Ridge regression is a linear method designed to deal with a high dimensionality of predictors (in our case many correlated spatial locations with streamfunction values, Φ_j). Ridge regression mitigates overfitting by introducing a penalty for model complexity, achieved through the shrinkage of regression coefficients. Shrinkage is determined by the sum of squared regression coefficients (known as L2 regularization) and a ridge regression parameter (λ), which controls the degree of shrinkage. The shrinkage term is added to the residual sum of squares (RSS) for the minimization:

$$\hat{\gamma} = \underset{\gamma}{\operatorname{argmin}} \{RSS + \lambda \sum_{i=1}^{p} \beta_i^2\}. \tag{3}$$

As a result, ridge regression solves a joint minimization problem, producing small but nonzero regression coefficients that are relatively evenly distributed among correlated predictors. The tuning parameter λ, which dictates the extent of shrinkage, is selected via cross-validation. Notably, the intercept of the linear model as well as the GMST covariate remain are excluded from the shrinkage.

2.3.2 Constructed atmospheric circulation analogues technique

The atmospheric circulation analogue technique, introduced in Deser et al. (2016), is a linear dynamical adjustment method designed to provide empirically derived estimates of climate trends induced by "dynamics" or atmospheric circulation patterns.

https://doi.org/10.5194/egusphere-2025-2397
Preprint. Discussion started: 4 June 2025

The method has been used for a variety of applications, including trend assessments, variability analysis, performance weighting, and extreme event attribution (Deser et al., 2016; Lehner et al., 2017; Merrifield et al., 2017; Guo et al., 2019; Merrifield et al., 2020; Terray, 2021).

The method is based on the construction of monthly mean atmospheric circulation fields, which we represent using sea level pressure (SLP) following Deser et al. (2016). Here, SLP analogues are selected from pools of N_a = 80 possible choices sub-selected from the period 1850-2014. From the 80 choices, N_s = 50 SLP analogues are selected to construct the target month, and the process is repeated N_r = 100 times to obtain an average best estimate result.

Once the Euclidean distances are determined and 50 of the 80 possible SLP analogues are selected, we optimally reconstruct a target SLP field $\mathbf{X}_h$ through a multivariate linear regression. The weight assigned to each SLP analogue, β, is computed through a singular value decomposition of a column vector matrix $\mathbf{X}_c$ containing the 50 selected analogues and can also be estimated using a Moore-Penrose pseudoinverse:

$$\beta = [(\mathbf{X}_c^T \mathbf{X}_c)^{-1} \mathbf{X}_c^T] \mathbf{X}_h \tag{4}$$

β weights are then applied to monthly mean temperature fields from the same months as the SLP analogues to construct the dynamic component. Before weighting the temperature fields, we remove a quadratic trend from the temperature record as a proxy for anthropogenic warming at each point in space (Deser et al., 2016; Lehner et al., 2017). This is to approximate the unforced relationship between SLP and temperature one would expect to find in a preindustrial control simulation. After repeating the dynamical adjustment protocol 100 times, we average the results to define a dynamic monthly mean temperature timeseries.

We use the term “analogue" to refer to a month with an SLP field close, in terms of Euclidean distance, to the SLP target. Here, Euclidean distance is computed at each grid point and averaged over the Northern hemisphere domain (20–90 °N, 0–360 °E). This selection metric, therefore, does not require an analogue to match the target month spatially over the whole domain. This is necessary because, with less than 200 possible options, it is extremely unlikely that a “perfect" match will exist for a particular target month. Van Den Dool (1994) estimated that around 10^{30} years would be required to find two similar (within observational uncertainty) Northern Hemisphere circulation patterns. Therefore, the method must make the best use of imperfect analogues, which may introduce spurious features or affect the amplitude of estimated dynamic temperature trends.

Two analogue pool selection strategies are employed. The first is an in-sample selection referred to as the “leave-one-out" approach (Lehner et al., 2017); analogues are selected from the CESM piC-nudged run being dynamically adjusted excluding the target month during the 1850-2014 period. The second is an out-of-sample approach; analogues are selected from the entire 1850-2014 periods of each of the other CESM piC-nudged runs and averaged. For example, run 1 is dynamically adjusted using analogues from run 2, then dynamically adjusted using analogues from run 3, and the two dynamic components are averaged. For ERA5, analogues are selected from all three CESM piC-nudged runs.

https://doi.org/10.5194/egusphere-2025-2397
Preprint. Discussion started: 4 June 2025

2.3.3 DEA

Direct Effect Analysis (DEA) is a recently developed causal approach that aims at disentangling an outcome variable Y into a direct effect component, Y_{dir}, which represents the part of Y directly caused by some causal factor Z, and an orthogonal component, Y_{perp}, which corresponds to the part of Y unaffected by Z. Both Z and Y may be influenced by other variables X, which act as confounders, and it is thus necessary to control for these covariates to get a correct estimate of direct effect of Z on Y. This learned representation of Y can be seen as the result of encouraging conditional independence between Z and Y while controlling for X (Durand et al., 2025)[1].

In this context, the outcome Y is the temperature field (a random vector where each dimension corresponds to a grid cell), and it is caused by Z, the GMST (monthly averaged), used as a proxy for thermodynamical changes in temperature. We consider as covariates X the leading Empirical Orthogonal Functions (EOFs) of the atmospheric circulation (Z500), denoted as $\{p_j\}_{j=1}^{J}$.

Similar to the ridge regression approach described above, we assume the following linear model:

$$Y = \gamma_0 + \mathbf{b}_0 \text{GMST} + \sum_{j=1}^{J} \mathbf{b}_j p_j + \epsilon. \tag{5}$$

and get the optimal regression parameter matrix using a least squares algorithm. We obtain a matrix $\mathbf{B}$ whose columns $\mathbf{b}_i$ encode how GMST and each EOF influence temperature across grid cells. We emphasize that this is a multivariate regression problem, where Y is a random vector—not a single variable—representing temperature values across multiple grid cells. Each dimension of Y corresponds to one spatial location. The number J of EOFs is selected through 5-fold cross-validation to maximize the $R2$ score.

To isolate the dynamical component Y_{perp} of Y, we remove the part aligned with the GMST-related direction, as captured by $\mathbf{b}_0$. This is achieved using the linear transformation $Y_{\text{perp}} = \mathbf{P}^\top Y$, where $\mathbf{P} = \mathbf{I} - \frac{\mathbf{b}_0 \mathbf{b}_0^\top}{\|\mathbf{b}_0\|^2}$. This transformation ensures that Y_{perp} remains unaffected by any interventions on GMST, and thus represents the dynamical component of Y.

2.3.4 UNET

The final method used in this paper is a convolutional neural network, a UNET structure, recently proposed by Cariou et al. (2025) to link temperature variations to atmospheric circulation. The UNET has been first introduced by Ronneberger et al. (2015) for biomedical image segmentation. It consists of two main parts: the encoder, which captures the global features of the input (here circulation maps) by progressively reducing its resolution while increasing the depth of the feature maps via convolution and max-pooling layers, and the decoder, which reconstructs the image using transposed convolutions. These two parts are symmetrical and connected by skip connections, enabling the network to preserve the encoded information.

We use this architecture (see C1) to estimate the relationship between daily sea-level pressure (SLP) maps (input) and the corresponding temperature anomalies (output):

$$T' = F(SLP) \tag{6}$$

[1] Accepted in UAI 2025.

https://doi.org/10.5194/egusphere-2025-2397
Preprint. Discussion started: 4 June 2025

We follow the methodology described in Cariou et al. (2025), using temperature anomalies obtained by removing an estimate of the daily non-stationary normal (Rigal et al. (2019)). SLP is not detrended assuming that the forced response of the circulation is small. In this study, we extend the analysis to a larger spatial domain and train the UNET on daily data from 1850 to 2100 from 8 CESM2 transient simulations (80% of the data are randomly selected for training and the remaining 20% are used for validation). The trained model is then tested on three CESM2 piC-nudged runs, with SLP maps standardized using the same values as in the training process.

For ERA5, we use the UNET previously trained on CESM2 and we train it again on ERA5 data from 1940 to 1978. This process is known as a fine-tuning method. SLP maps are standardized with mean and standard deviation calculated on this training period and the non-stationary normal is computed thanks to an estimate of the forced response obtained with Qasmi and Ribes (2022) method. Then we test it over the 1979-2023 period.

3 Results and Discussion

In the following, we evaluate each statistical method's estimate of circulation-induced mid-latitude JJA temperature trends. To obtain those estimates, each statistical method is applied to obtain a circulation-induced temperature estimate from the CESM2 free-running hist+ssp370 climate change simulations, and subsequently evaluated against the piControl-nudged CESM2 simulations, which is used as a benchmark. The skill of each method is assessed by calculating four skill metrics: (i) the fraction of correctly identified signs, (ii) Pearson correlation, that is a pattern correlation across the mid-latitudes, (iii) the coefficient of determination (R^2 score, that is the proportion of variance of circulation-induced trends captured by the statistical predictions), (iv) the regression slope between the predicted and benchmark trend estimates.

(i) This metric provides a general sense of whether the method can correctly capture the sign of the trend, which may be sufficient in certain contexts—for example, in climate change detection. (ii) Pearson correlation reflects how well the method captures the spatial pattern of the trend. Some methods may systematically over- or underestimate the magnitude of trends, yet still accurately reproduce their spatial distribution. (iii) The coefficient of determination (R^2) is a widely used metric for spatial comparisons, as it accounts for the variance at each location and indicates how much of the observed variability is explained by the prediction. (iv) The regression slope indicates whether the method tends to overestimate or underestimate the magnitude of trends.

3.1 Evaluation of circulation-induced trends in the historical period (1979-2023) in CESM2 nudged-circulation simulations

Over the period 1979-2023 JJA temperature trends in the piControl-nudged simulations range from -0.35 to 0.35 K per decade (figure 3 a,d,g). These trends are organized in large regional clusters of alternating signs. Furthermore, the trend patterns differ considerably between the three piControl-nudged runs indicating that in CESM2 circulation induced trends are dominated by internal variability and that in CESM2 forced circulation changes are small. Overall, JJA temperature trends are slightly higher in run 1 which is likely due to the positive GMT trends in the piControl-nudged runs during this period (see figure 2).

https://doi.org/10.5194/egusphere-2025-2397
Preprint. Discussion started: 4 June 2025

Table 1. Evaluation metrics comparing trends in piControl-nudged simulations to estimates of circulation induced trends from statistical decomposition methods for land grid-cells between 30N-60N and the period 1979-2023. First block: percentage of correctly predicted sign. Second block: Pearson correlation coefficient. Third block: Coefficient of determination. Fourth block: regression slope. See table D1 for the same evaluation over the period 2025-2075.

run	ridge	analogues	DEA	UNET
	correct sign			
all runs	**75%**	**65%**	**76%**	**84%**
run 1	76%	77%	73%	86%
run 2	74%	56%	82%	84%
run 3	76%	63%	73%	83%
	Pearson correlation			
all runs	**0.74**	**0.52**	**0.64**	**0.86**
run 1	0.79	0.57	0.61	0.91
run 2	0.65	0.36	0.74	0.83
run 3	0.75	0.41	0.58	0.89
	R2			
all runs	**0.53**	**0.07**	**0.10**	**0.66**
run 1	0.56	0.18	-0.20	0.50
run 2	0.39	-0.28	0.25	0.67
run 3	0.47	-0.07	-0.04	0.73
	regression slope			
all runs	**0.65**	**0.43**	**0.73**	**0.51**
run 1	0.59	0.47	0.70	0.47
run 2	0.51	0.26	0.96	0.57
run 3	0.54	0.36	0.65	0.58

Next, we discuss the performance of each statistical method. Using the ridge regression trained on a forced simulation to predict the trends based on the streamfunction of the forced simulation and the GMT of the piControl-nudged run, we get a similar trend pattern as in the piControl-nudged run (figure 3 b,e,h). Over the mid-latitudinal land area, half of the variability in local temperature trends in the piControl-nudged run is explained by the ridge regression model (compare R2 score in table 1). For three quarters of the grid-cells the sign of the predicted trend is correct and grid-cells for which the sign of the trend is not predicted correctly are mostly grid-cells with small trends in the piControl-nudged simulation (and the prediction).

https://doi.org/10.5194/egusphere-2025-2397
Preprint. Discussion started: 4 June 2025

The analog method also shows a positive correlation between predicted and simulated mid-latitude land trends and a similar percentage of correctly predicted signs of trends for run 1 and slightly lower performance for the two other runs. Note that in the analogues method we estimate the trend contribution coming from circulation and cannot account for contributions of GMST changes in the piControl-nudged simulation. It is therefore expected that the results are worse for run 2 and run 3 where a considerable negative trend in GMST was simulated in the piControl-nudged runs.

The DEA method performs well in estimating the sign of circulation induced trends (76% correct; see table 1). Despite the relatively good correlation between the trend maps (0.64) the coefficient of determination is close to zero. Estimates of circulation induced trends from DEA cover the full range of simulated piControl-nudged trends including very high and very low trends. This is reflected by a relatively high regression slope between predicted and simulated trends (figure B1 and last block in table 1).

The UNET is performing best of all tested methods here. With UNET, 84% of trends signs are predicted correctly, it has the highest Pearson correlation coefficient (0.86) and the highest coefficient of determination (0.66). As compared to the DEA and the ridge regression, UNET has a tendency to predict lower circulation induced trends and rarely exceeding magnitudes of 0.2 K per decade. As shown in figure B1d this leads to a systematic underestimation of the trend magnitude compared to the piControl-nudged simulation.

The evaluation over a different period (2025-2075) leads to similar skill metrics and confirms the above discussed results (see figure D1 and table D1).

Overall, UNET is the most accurate method when it comes to explain the variance in mid-latitude boreal summer temperature trends. The ridge regression and UNET have the tendency to decompose the temperature trends into a regionally smoothed pattern of circulation-induced temperature trends and have a lower likelihood of predicting a strong trend of wrong sign. DEA and the analogue method project strong trends of wrong sign in some regions. DEA appears to be more useful when it comes to estimate the potential magnitude of circulation-induced trends while UNET is rather conservative and estimates generally to weak trends. The analogue method also shows skill in predicting the sign of trend but appears generally less trustworthy when it comes to circulation-induced trends.

https://doi.org/10.5194/egusphere-2025-2397
Preprint. Discussion started: 4 June 2025

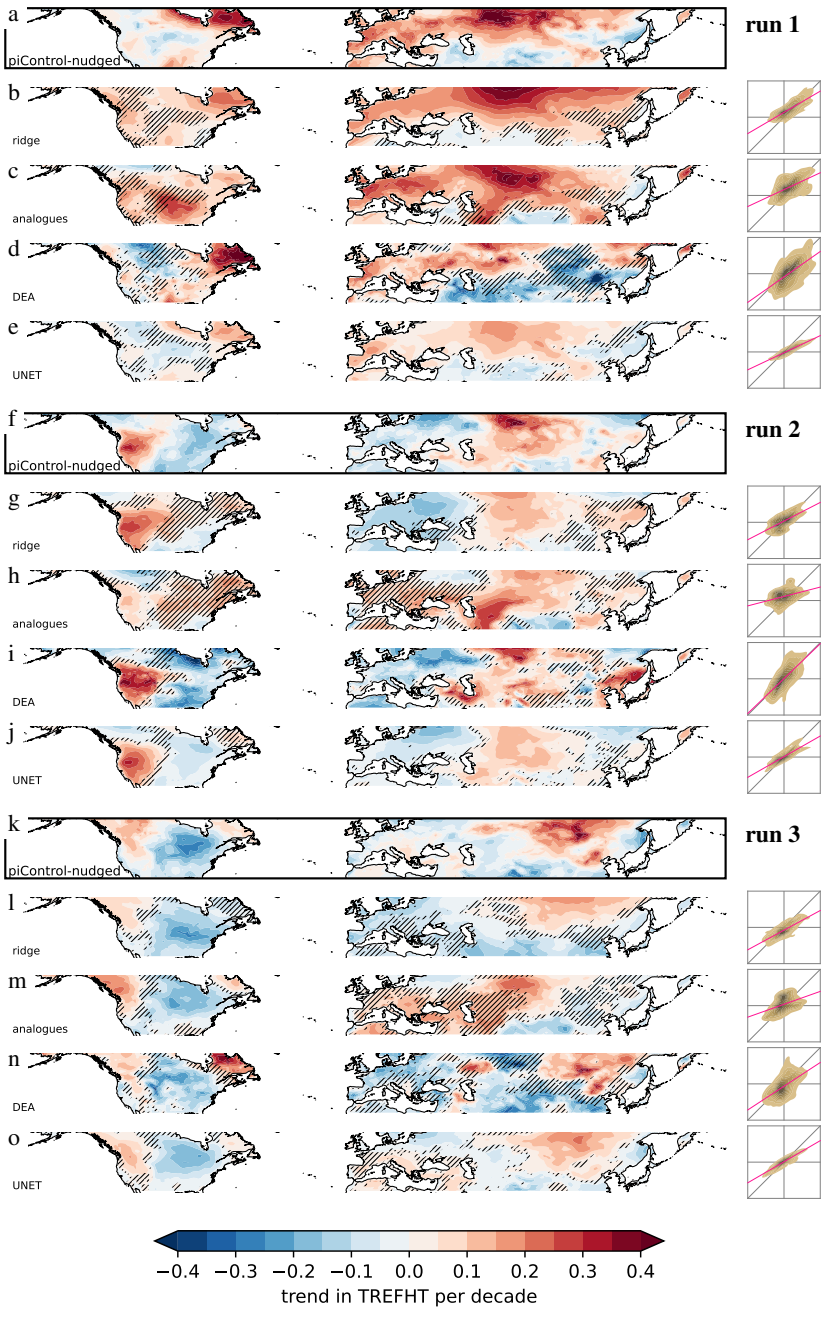

Figure 3. Trend in JJA temperatures over the period 1979-2023 in piControl-nudged (a,f,k) and predicted trends from different decomposition methods. For the run 1 (a-e), 2 (f-j) and 3 (k-o). Estimates from the ridge regression (b,g,l), the analogues (c,h,m), DEA (d,i,n) and UNET (e,j,o). Areas where the predicted trend differs in sign from the piControl-nudged run are highlighted by black hatching. Besides the estimated trend maps from decomposition methods, small kernel density estimates of estimated trends (y-axis) versus simulated piControl-nudged trends (x-axis) are shown with x- and y-axis ranging from -0.5 K/dec to 0.5 K/dec.

https://doi.org/10.5194/egusphere-2025-2397
Preprint. Discussion started: 4 June 2025

3.2 Identification of the circulation-induced boreal summer temperature trend (1979-2023) in reanalysis

All decomposition methods applied to the ERA5 reanalysis as well as the CESM2 simulations nudged to ERA5 winds suggest similar circulation induced trend patterns for the period 1979-2023: Over Eurasia, a wave-like trend pattern for the circulation induced trends is apparent with strong positive trends over Central and Eastern Europe (around 30E), cooling trends over Kazakhstan and western Siberia (between 60E and 90E), and warming trends over Mongolia, eastern Siberia and Central China (between 90E and 120E), and extending towards the Kamchatka peninsula (Fig. 4). Over North America we find a dipole pattern with positive trends over the western part and negative trends over the center and eastern parts; with positive trends in the outermost north-eastern parts again. All decomposition methods as well as the CESM2 simulations nudged to ERA5 winds (figure 4j) agree on this broad trend pattern with only little regional deviations. The trend pattern identified with the statistical method is in good agreement with the pattern found in Teng et al. (2022).

From our evaluation of decomposition methods against dedicated nudged experiments in the CESM2 setup we would suggest to give more weight to the results from UNET when it comes to the sign of circulation induced trends. For example, this would imply that the positive circulation induced trends over northern North America in the ridge regression are probably wrong (compare low skill of ridge regression in this region, figure 3).

Moreover, there remains ambiguity on the magnitude of the above described trend pattern. The ridge regression, DEA and UNET suggest a circulation induced trend of up to 0.3 K/dec over eastern Europe while the piControl simulations from CESM2 that where nudged to ERA5 winds stronger circulation induced trends of up to 0.6 K/dec. In other regions, the nudged simulations and DEA have stronger trends followed by the ridge regression and analogues and UNET suggest somewhat weaker trends. From the evaluation of the decomposition methods we know that all methods except DEA have indeed a tendency of somewhat underestimating the magnitude of circulation induced trends suggesting that the circulation induced trend over eastern Europe could be around 0.5 K/dec as suggested by the nudged simulations and DEA.

In summary, our study confirms the highly variable mid-latitude boreal summer trend pattern found in Singh et al. (2023); Teng et al. (2022); Vautard et al. (2023) with five independent methods (four statistical methods and a nudged circulation simulation driven by ERA5 horizontal wind fields). The trend pattern contains substantial regional warming hotspots in all of which a positive circulation contribution to warming has played a key role Teng et al. (2022). It is important to note that while the total boreal summer temperature trends are positive all over the NH mid-latitudes, circulation has contributed with cooling temperatures in large regions, in particular Central and Eastern North America, Central Eurasia, and to a minor extent coastal eastern China. Moderately positive total trends in those regions are therefore due to a compensation of the circulation-induced cooling by a positive thermodynamic contribution.

3.3 Implications and limitations of statistical methods to isolate circulation effects on the time scales of climate trends

Many previous studies aimed to identify circulation-induced components in time series of climate variables, a methodology which is sometimes framed as ‘dynamical adjustment’ (Smoliak et al., 2015; Deser et al., 2016; Guo et al., 2019; Cariou et al., 2025; Singh et al., 2023; Saffioti et al., 2017; Lehner et al., 2017). The main idea is that circulation variability dominates

https://doi.org/10.5194/egusphere-2025-2397
Preprint. Discussion started: 4 June 2025

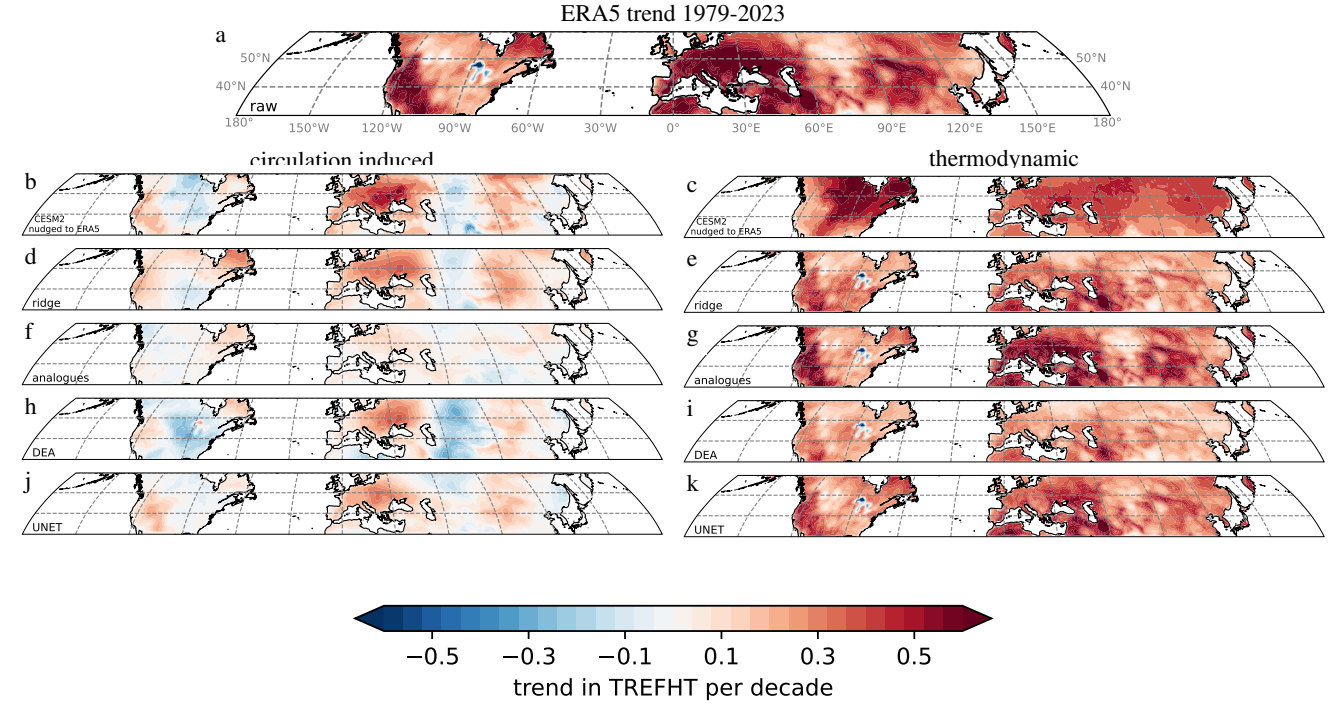

Figure 4. JJA mean temperature trends in ERA5 over the period 1979-2023 (a) decomposed in the circulation-induced (left) and thermodynamic (right) contribution for the ridge regression (d,e), DEA (f,g), analogues (h,i), UNET (j,k) and estimates from CESM2 simulation with horizontal winds nudged to ERA5 winds (b,c).

temperature variability in many regions of the world and is dominated by internal variability; thermodynamic contributions are obtained as a residual (e.g. Deser et al., 2016). The identification and separation of climate time series into dynamic and thermodynamic is a powerful tool for attribution (e.g. Shepherd, 2014).

However, while different statistical methods to obtain the circulation-induced components in climate time series are routinely evaluated on short time scales, the estimation of circulation-induced decadal trends has remained a challenge for the climate community and will likely remain one. This is because of five main reasons.

First, statistical methods have been found to perform very well on short time scales of day-to-day, month-to-month or inter-annual variability (Cariou et al., 2025; Smoliak et al., 2015; Sippel et al., 2019). Yet, the difference in the performance on long (that is, trend) time scales versus short time scales has not been quantified so far, although dynamical adjustment has been widely applied on the time scales of trends. A reduced performance on long time scales is expected, and indeed found in this study, because shorter time scales are dominated to the largest extent by circulation-induced variability, whereas on longer time scales other processes are becoming more dominant, such as land-atmosphere interactions (e.g. Merrifield et al., 2017) or long-term warming, both of which may not be straightforward to account for.

https://doi.org/10.5194/egusphere-2025-2397
Preprint. Discussion started: 4 June 2025

Second, and partly related to the previous point, designing a method comparison for the identification of circulation-induced time series is challenging. This is because it is not immediately apparent what the components are that the signal is decomposed to; and which relevant mechanisms can be attributed to these components. In this study, we decompose a trend in local temperatures into a "circulation induced" component and a thermodynamic component without specifying to which of these component changes in other important factors, such as soil-moisture or aerosol concentrations, are attributed to. The different statistical methods evaluated here were initially developed for similar but slightly different research questions: The analogue method, for instance, was designed to separate the "thermodynamic signal" from "circulation-induced variability". Yet, it has been shown that summer land-atmosphere interactions remain largely in the residual, thermodynamic component due to the way that the method is set up (Merrifield et al., 2017). On the other hand, machine learning methods such as the UNETs may partly implicitly identify land-atmosphere interactions as part of circulation variability, if circulation carries an imprint of land-atmosphere variability.

Third, it is not straightforward to design a benchmark for the circulation-induced component in time series of climate variables, such as summer temperatures. Here, we have used a pi-control nudged-circulation approach as a benchmark, where a climate model was nudged to the horizontal winds of a forced, transient simulation. We thus obtain circulation-induced changes in an unforced climate simulation. However, there may be factors of residual climate variability (such as ocean variability) or feedbacks between circulation and other factors such as land-atmosphere coupling that could still affect thermodynamical processes on climate over land. However, based on the similarity between the pi-control nudged circulation simulations and the statistical methods, the climate model based benchmark is valid for our purpose.

Fourth, we present an evaluation of decomposition methods based on one set of nudged simulations from one earth system model (CESM2). Although the well documented performance of CESM2, this is a flaw as the strength of the links between atmospheric circulation patterns, GMST and local temperatures might be misrepresented in the model. A followup study using multiple ESMs to create a benchmarking dataset would be crucial to further constrain our estimates of circulation induced temperature trends. The use of such a multi-model ensemble would require to slightly adapt the different reconstruction methods. In particular the UNET would have to be pre-trained on a collection of multi-model data, instead of just CESM2. Preliminary tests done on Western Europe suggest that this does not degrade the quality of the reconstruction, especially when we add the fine-tuning step on early ERA5 data.

Finally, besides combining multiple lines of evidence, our study highlights the need of benchmarking efforts for statistical and machine learning approaches: without the evaluation against nudged circulation simulations one would conclude that different decomposition methods project similar trend patterns with some estimates showing a stronger version of the trend pattern than others. Evaluating which magnitude of the trend pattern is the most likely/plausible is challenging from the statistical analysis alone. Concluding that all decomposition methods applied to observations might be underestimating the magnitude of the trend pattern would be impossible.

Overall, our study shows that statistical methods are well-suited to identify and separate circulation-induced temperature trends from residual, thermodynamical trends. It is important to note, however, that the performance of those methods on time scales of climatic trends decreases relative to the higher performance found on short time scales. It is therefore crucial to

https://doi.org/10.5194/egusphere-2025-2397
Preprint. Discussion started: 4 June 2025

account for this kind of uncertainty in potential subsequent studies that would use those estimates for attribution of to derive constraints on future projections.

4 Conclusions and Outlook

In summary, our analysis targeted two specific research objectives and revealed two distinct findings: First, we evaluated whether statistical-empirical methods are able to correctly estimate circulation-induced long-term trends in the NH mid-latitudes in boreal summer (and a residual that is dominated by thermodynamic trends) against a specifically designed climate model benchmark of nudged circulation experiments. Four different statistical methods were tested and we showed that each of these methods is able to identify in general the large-scale pattern of circulation variability and changes, even though the methods are typically trained and validated on short time scales (daily to seasonal). However, methods showed differences in their skill in which they reproduced the spatial trend pattern from the nudged circulation benchmark, and in the extent to which they partly underestimated the magnitude of circulation trends: With three quarters of correctly estimated signs of trends and coefficients of determination above 50%, the ridge regression and the UNET methods are performing sufficiently well for the purpose. The UNET has overall the highest scores in most tested skill metrics. However, the UNET method tends to produce underdispersive results, that is the magnitude of particularly strong circulation trends is often underestimated (irrespective of the sign). DEA and circulation analogues have similar skill in predicting the sign of circulation-induced trends, but due to the low coefficient of determination we would restrain from interpreting the magnitude of regional trends estimated from these methods. Overall, identifying circulation-induced trends on climate time scales in the context of dynamical adjustment studies is possible, but it does imply larger uncertainties than for the application on shorter time scales, which needs to be considered in future applications of the techniques.

Our second objective was to identify circulation-induced boreal summer temperature trends across the northern hemispheric mid-latitudes in observations using four different statistical methods and CESM2 simulations that are nudged to the ERA5 circulation without anthropogenic forcing. Large-scale boreal summer circulation trends and their effects on temperature have been a topic of intense discussion (Teng et al., 2022; Chemke and Coumou, 2024; Rousi et al., 2022; Vautard et al., 2023). Our analysis of circulation induced trends in ERA5 over the period 1979-2023 confirms the positive circulation contribution to summer heat over Europe, Western North America, and over Mongolia. Following a wave pattern, circulation-induced cooling has been identified over Central Eurasia (Western Siberia and Kazakhstan) and Central and Eastern North America.

Besides adding to the confidence in circulation induced temperature changes, our evaluation also raises awareness about systematic shortcomings of statistical decomposition methods. A better understanding of the performance of decomposition methods could improve our ability to attribute regional climate trends. Attribution of individual components of historical changes is likely to identify a stronger signal, especially when it comes to the attribution of regional climate change. Focusing on dynamical and thermodynamical changes separately is an advantage as there are great differences in the uncertainties of forced changes in these components (Shepherd, 2014). While several attribution studies of circulation changes have been published (Coumou et al., 2015; Chemke and Coumou, 2024; Dong et al., 2022); uncertainties remain large especially when it

https://doi.org/10.5194/egusphere-2025-2397
Preprint. Discussion started: 4 June 2025

comes to the attribution of the downstream impacts of atmospheric circulation changes. Being able to more robustly decompose a trend into a circulation-induced and a thermodynamic component should also help to better attribute circulation-induced temperature trends.

Finally, the separation into dynamical and thermodynamic components could be used to constrain projections of the near future using observation-based constraints. The thermodynamic constraint should be straight forward to identify as it is mainly forced. There are different possibilities to constrain based on the dynamical component: with the assumption that circulation-induced trends over the past decades were largely due to internal climate variability one would expect a reversal of the trend pattern observed over the coming decades. If circulation-induced temperature change is forced, both circulation-induced and thermodynamical trends would continue into the future. Due to the large uncertainty in the forced circulation-induced changes a storyline approach would be appropriate, explicitly treating different assumptions about forced atmospheric circulation changes and evaluating the potential outcomes of these scenarios (Shepherd, 2019; Liné et al., 2024).

Code and data availability. The code required to reproduce this study is available on https://github.com/peterpeterp/circ_contribution_to_JJA_trends.git.

https://doi.org/10.5194/egusphere-2025-2397
Preprint. Discussion started: 4 June 2025

Appendix A: Nudged circulation plots

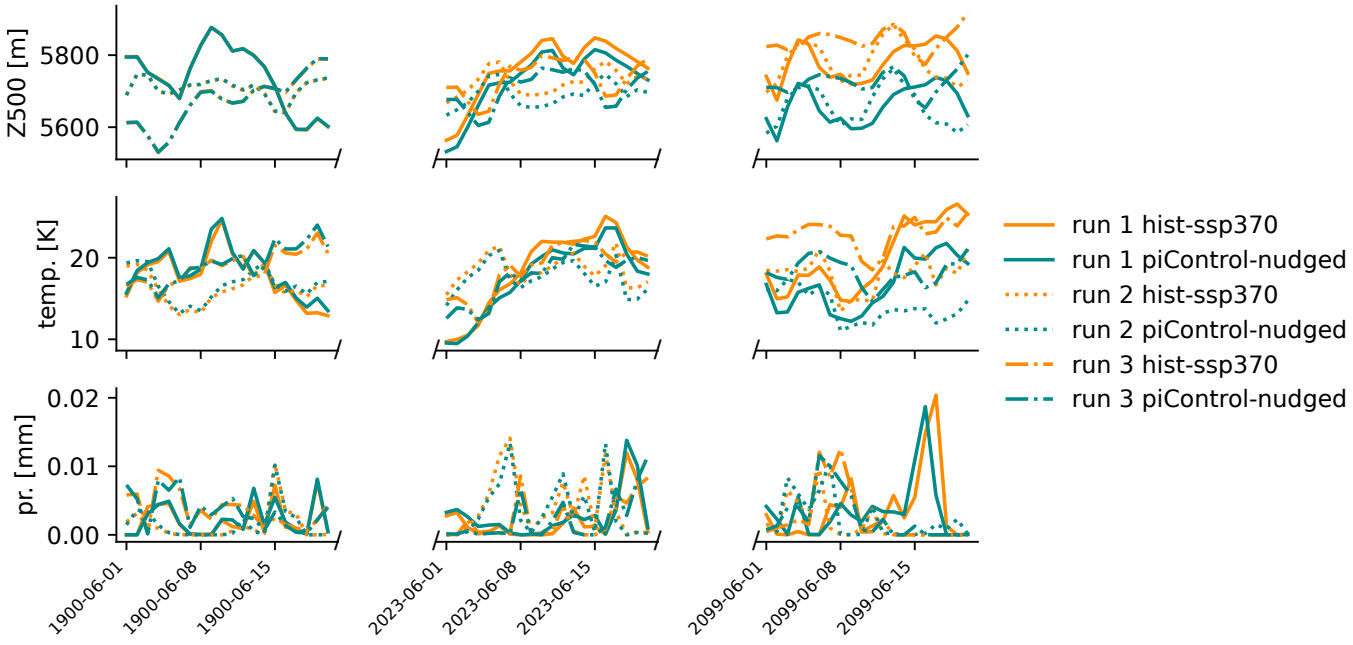

Figure A1. Differences in temperature, precipitation and geopotential height at 500hPa at one grid-cell (next to Leipzig). Orange lines represent hist+ssp370 simulations, green lines represent the corresponding piControl-nudged simulations.

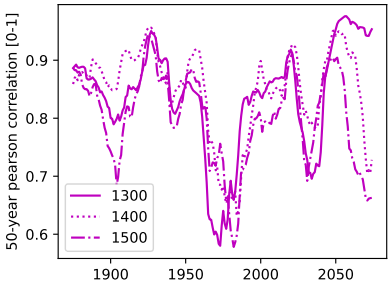

Figure A2. 50-year running correlation between hist+ssp370 and piControl-nudged run.

https://doi.org/10.5194/egusphere-2025-2397
Preprint. Discussion started: 4 June 2025

Appendix B: More evaluation plots

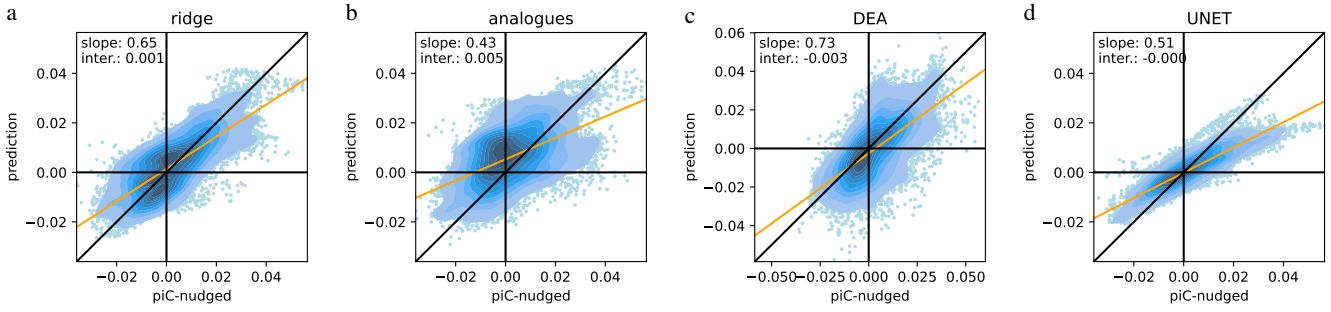

Figure B1. Predicted trends against trends from piControl-nudged for the period 1979-2023 over land grid-cells between 30N and 60N from all runs (1,2,3) for the ridge regression (a), DEA (b), analogues (c) and UNET (d). The bulk of the data is represented by a gaussian kernel density estimate (shadings) while extreme trends are shown as scatter points.

https://doi.org/10.5194/egusphere-2025-2397
Preprint. Discussion started: 4 June 2025

Appendix C: UNET architecture

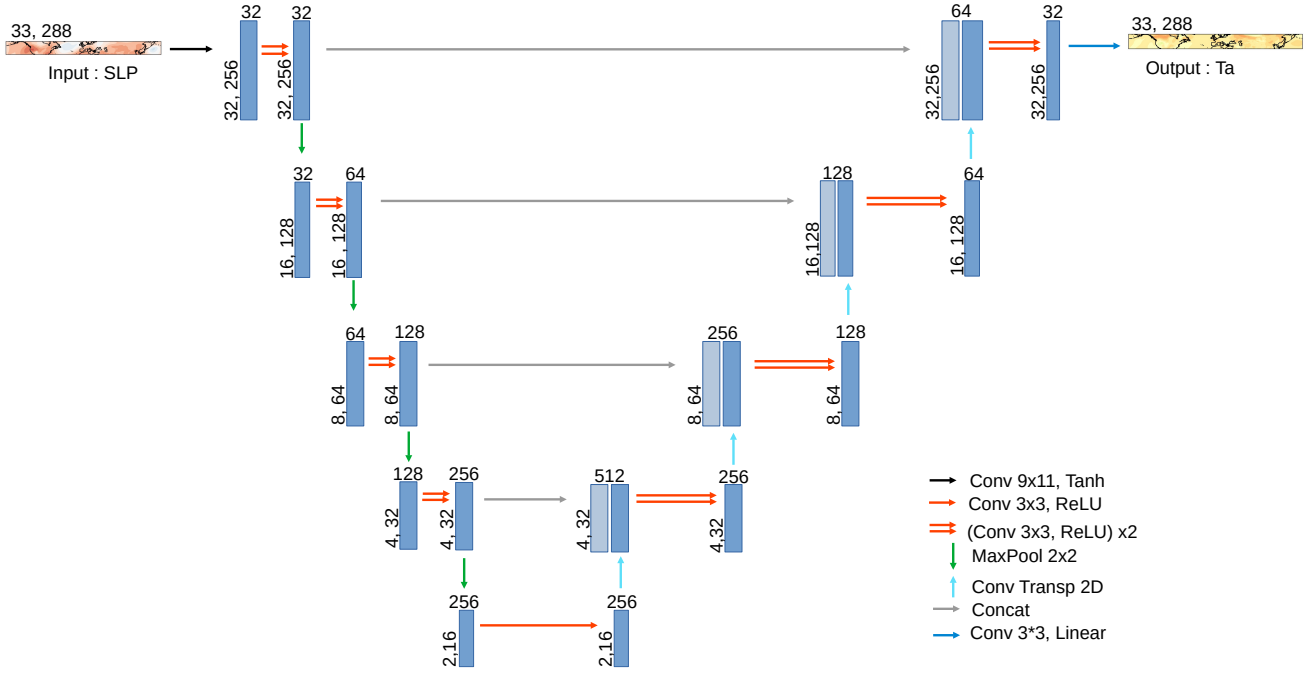

Figure C1. UNET architecture.

Appendix D: Period 2025-2075

https://doi.org/10.5194/egusphere-2025-2397
Preprint. Discussion started: 4 June 2025

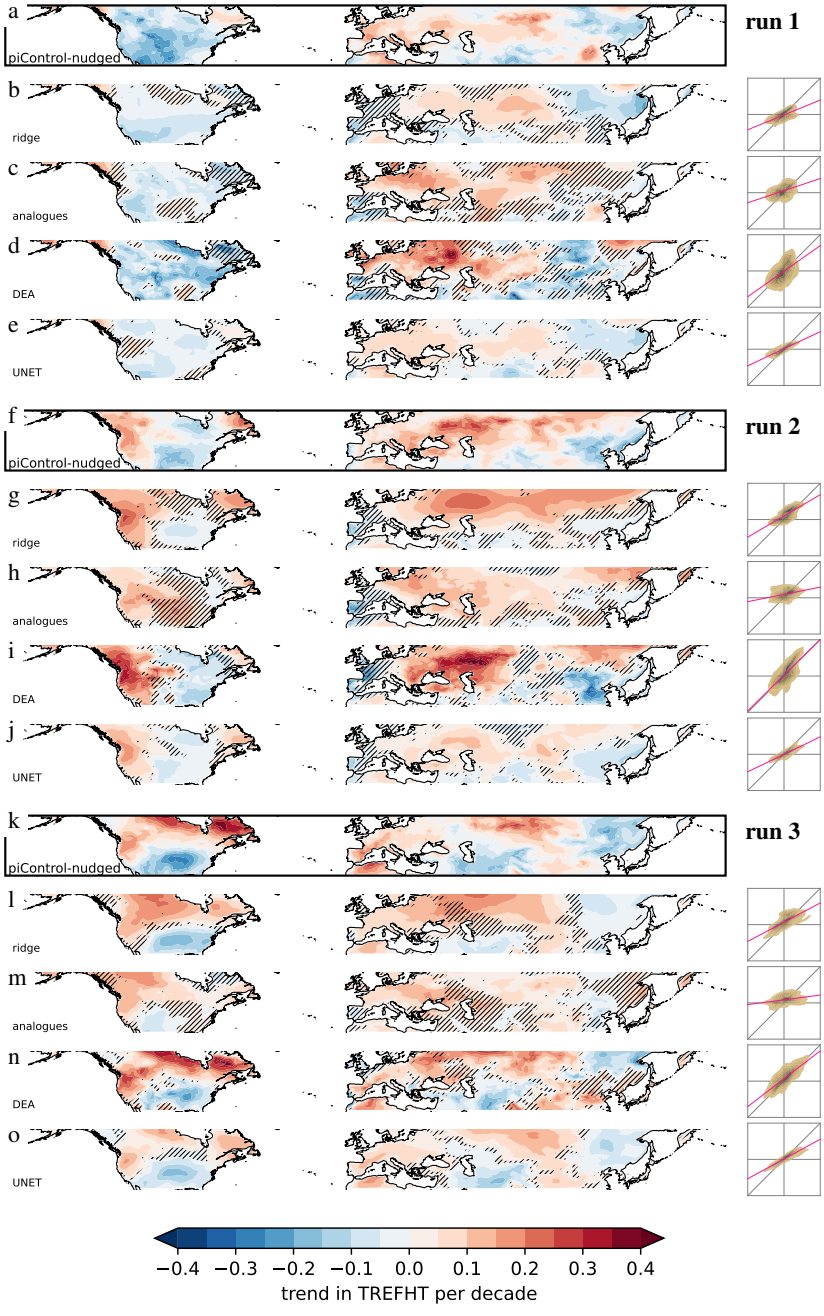

Figure D1. Same as figure 3 but for the period 2025-2075.

https://doi.org/10.5194/egusphere-2025-2397
Preprint. Discussion started: 4 June 2025

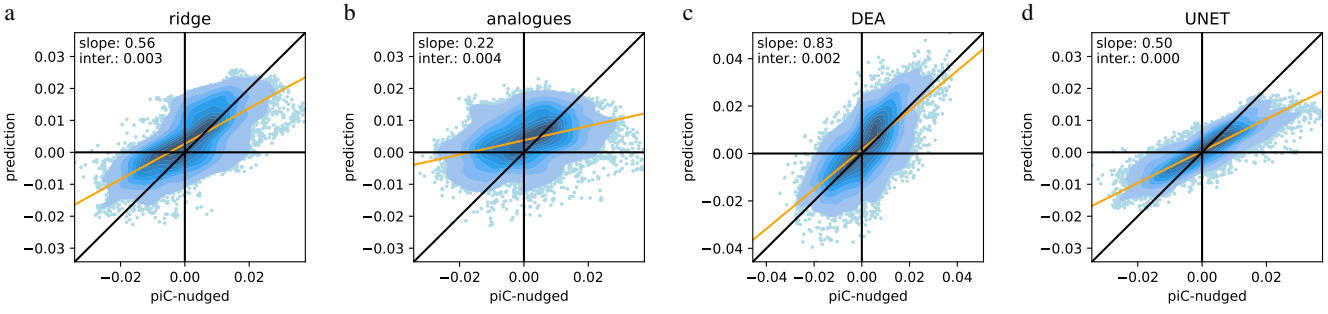

Figure D2. Same as figure B1 but for the period 2025-2075.

https://doi.org/10.5194/egusphere-2025-2397
Preprint. Discussion started: 4 June 2025

Table D1. Same as table 1 but for the period 2025-2075.

run	ridge	analogues	DEA	UNET
	correct sign			
all runs	**77%**	**65%**	**78%**	**87%**
run 1	73%	63%	74%	87%
run 2	76%	68%	80%	85%
run 3	81%	64%	81%	89%
	Pearson correlation			
all runs	**0.70**	**0.37**	**0.70**	**0.86**
run 1	0.62	0.44	0.55	0.82
run 2	0.72	0.31	0.73	0.83
run 3	0.73	0.29	0.79	0.91
	R2			
all runs	**0.44**	**-0.00**	**0.23**	**0.66**
run 1	0.38	-0.09	-0.24	0.58
run 2	0.35	-0.07	0.14	0.60
run 3	0.49	0.00	0.53	0.73
	regression slope			
all runs	**0.56**	**0.22**	**0.83**	**0.50**
run 1	0.41	0.33	0.71	0.47
run 2	0.59	0.20	0.99	0.48
run 3	0.53	0.13	0.77	0.54

https://doi.org/10.5194/egusphere-2025-2397
Preprint. Discussion started: 4 June 2025

Author contributions. PP and SS conceived the study. PP wrote the manuscript with contributions from SS and all other authors. PP created all figures. PP contributed the results of the ridge regression. AM contributed the results for the constructed analogues. HD contributed the results for DEA. EC and JC contributed the results for UNET. ID contributed the CESM2 simulations nudged to ERA5 winds.

Competing interests. No competing interests are present.

Acknowledgements. We thank Urs Beyerle for producing the nudged CESM2 simulations that were used to evaluate the statistical decomposition methods. We thank all the scientists, software engineers, and administrators who contributed to the development of CESM. We acknowledge the use of ERA5 reanalysis data provided by the Copernicus Climate Change Service (C3S). We acknowledge the CESM2 Large Ensemble Community Project for providing the model output used in this study. S.S. and P.P. acknowledge the project 'Artificial Intelligence for Enhanced Representation of Processes and Extremes in Earth System Models' (AI4PEX; grant agreement 101137682), funded by the EU's Horizon Europe program; and the climXtreme project funded by the German Federal Ministry of Education and Research (Phase 2, project PATTETA, grant number 01LP2323C). S.S. and I.D. acknowledge funding from the German Research Foundation's Heinz Maier-Leibnitz Prize 2024 for early career researchers.

https://doi.org/10.5194/egusphere-2025-2397
Preprint. Discussion started: 4 June 2025

References

camdoc: Camdoc Documentation: 9 Physics Modifications via the Namelist, https://ncar.github.io/CAM/doc/build/html/users_guide/physics-modifications-via-the-namelist.html#nudging.

Cariou, E., Cattiaux, J., Qasmi, S., Ribes, A., Cassou, C., and Doury, A.: Linking European Temperature Variations to Atmospheric Circulation With a Neural Network: A Pilot Study in a Climate Model, Geophysical Research Letters, 52, e2024GL113 540, https://doi.org/10.1029/2024GL113540, 2025.

Cattiaux, J., Vautard, R., Cassou, C., Yiou, P., Masson-Delmotte, V., and Codron, F.: Winter 2010 in Europe: A Cold Extreme in a Warming Climate: COLD WINTER 2010 IN EUROPE, Geophysical Research Letters, 37, https://doi.org/10.1029/2010GL044613, 2010.

Chemke, R. and Coumou, D.: Human Influence on the Recent Weakening of Storm Tracks in Boreal Summer, npj Climate and Atmospheric Science, 7, 1–8, https://doi.org/10.1038/s41612-024-00640-2, 2024.

Coumou, D., Lehmann, J., and Beckmann, J.: The Weakening Summer Circulation in the Northern Hemisphere Mid-Latitudes, Science, 348, 324–327, https://doi.org/10.1126/science.1261768, 2015.

Danabasoglu, G., Lamarque, J.-F., Bacmeister, J., Bailey, D. A., DuVivier, A. K., Edwards, J., Emmons, L. K., Fasullo, J., Garcia, R., Gettelman, A., Hannay, C., Holland, M. M., Large, W. G., Lauritzen, P. H., Lawrence, D. M., Lenaerts, J. T. M., Lindsay, K., Lipscomb, W. H., Mills, M. J., Neale, R., Oleson, K. W., Otto-Bliesner, B., Phillips, A. S., Sacks, W., Tilmes, S., van Kampenhout, L., Vertenstein, M., Bertini, A., Dennis, J., Deser, C., Fischer, C., Fox-Kemper, B., Kay, J. E., Kinnison, D., Kushner, P. J., Larson, V. E., Long, M. C., Mickelson, S., Moore, J. K., Nienhouse, E., Polvani, L., Rasch, P. J., and Strand, W. G.: The Community Earth System Model Version 2 (CESM2), Journal of Advances in Modeling Earth Systems, 12, e2019MS001 916, https://doi.org/10.1029/2019MS001916, 2020.

Deser, C., Terray, L., and Phillips, A. S.: Forced and Internal Components of Winter Air Temperature Trends over North America during the Past 50 Years: Mechanisms and Implications*, Journal of Climate, 29, 2237–2258, https://doi.org/10.1175/JCLI-D-15-0304.1, 2016.

Dong, B., Sutton, R. T., Shaffrey, L., and Harvey, B.: Recent Decadal Weakening of the Summer Eurasian Westerly Jet Attributable to Anthropogenic Aerosol Emissions, Nature Communications, 13, 1148, https://doi.org/10.1038/s41467-022-28816-5, 2022.

Durand, H., Varando, G., and Camps-Valls, G.: Learning Causal Response Representations through Direct Effect Analysis, arXiv preprint arXiv:2503.04358, 2025.

Eyring, V., Gillett, N. P., Achuta Rao, K. M., Barimalala, R., Barreiro Parrillo, M., Bellouin, N., Cassou, C., Durack, P. J., Kosaka, Y., McGregor, S., Min, S., Morgenstern, O., and Sun, Y.: Human Influence on the Climate System, in: Climate Change 2021: The Physical Science Basis. Contribution of Working Group I to the Sixth Assessment Report of the Intergovernmental Panel on Climate Change, edited by Masson-Delmotte, V., Zhai, P., Pirani, A., Connors, S. L., Péan, C., Berger, S., Caud, N., Chen, Y., Goldfarb, L., Gomis, M. I., Huang, M., Leitzell, K., Lonnoy, E., Matthews, J. B. R., Maycock, T. K., Waterfield, T., Yelekçi, O., Yu, R., and Zhou, B., book section 3, pp. 463–466, Cambridge University Press, Cambridge, United Kingdom and New York, NY, USA, 2021.

Fabiano, F., Meccia, V. L., Davini, P., Ghinassi, P., and Corti, S.: A Regime View of Future Atmospheric Circulation Changes in Northern Mid-Latitudes, Weather and Climate Dynamics, 2, 163–180, https://doi.org/10.5194/wcd-2-163-2021, 2021.

Fereday, D., Chadwick, R., Knight, J., and Scaife, A. A.: Atmospheric Dynamics Is the Largest Source of Uncertainty in Future Winter European Rainfall, Journal of Climate, 31, 963–977, https://doi.org/10.1175/JCLI-D-17-0048.1, 2018.

Guo, R., Deser, C., Terray, L., and Lehner, F.: Human Influence on Winter Precipitation Trends (1921–2015) over North America and Eurasia Revealed by Dynamical Adjustment, Geophysical Research Letters, 46, 3426–3434, https://doi.org/10.1029/2018GL081316, 2019.

https://doi.org/10.5194/egusphere-2025-2397
Preprint. Discussion started: 4 June 2025

Hanna, E., Fettweis, X., and Hall, R. J.: Brief Communication: Recent Changes in Summer Greenland Blocking Captured by None of the CMIP5 Models, The Cryosphere, 12, 3287–3292, https://doi.org/10.5194/tc-12-3287-2018, 2018.

Hersbach, H., Bell, B., Berrisford, P., Hirahara, S., Horányi, A., Muñoz-Sabater, J., Nicolas, J., Peubey, C., Radu, R., Schepers, D., Simmons, A., Soci, C., Abdalla, S., Abellan, X., Balsamo, G., Bechtold, P., Biavati, G., Bidlot, J., Bonavita, M., De Chiara, G., Dahlgren, P., Dee, D., Diamantakis, M., Dragani, R., Flemming, J., Forbes, R., Fuentes, M., Geer, A., Haimberger, L., Healy, S., Hogan, R. J., Hólm, E., Janisková, M., Keeley, S., Laloyaux, P., Lopez, P., Lupu, C., Radnoti, G., de Rosnay, P., Rozum, I., Vamborg, F., Villaume, S., and Thépaut, J.-N.: The ERA5 Global Reanalysis, Quarterly Journal of the Royal Meteorological Society, 146, 1999–2049, https://doi.org/10.1002/qj.3803, 2020.

Horton, D. E., Johnson, N. C., Singh, D., Swain, D. L., Rajaratnam, B., and Diffenbaugh, N. S.: Contribution of Changes in Atmospheric Circulation Patterns to Extreme Temperature Trends, Nature, 522, 465–469, https://doi.org/10.1038/nature14550, 2015.

Kornhuber, K., Bartusek, S., Seager, R., Schellnhuber, H. J., and Ting, M.: Global Emergence of Regional Heatwave Hotspots Outpaces Climate Model Simulations, Proceedings of the National Academy of Sciences, 121, e2411258 121, https://doi.org/10.1073/pnas.2411258121, 2024.

Lehner, F., Deser, C., and Terray, L.: Toward a New Estimate of "Time of Emergence" of Anthropogenic Warming: Insights from Dynamical Adjustment and a Large Initial-Condition Model Ensemble, Journal of Climate, 30, 7739–7756, https://doi.org/10.1175/JCLI-D-16-0792.1, 2017.

Liné, A., Cassou, C., Msadek, R., and Parey, S.: Modulation of Northern Europe Near-Term Anthropogenic Warming and Wettening Assessed through Internal Variability Storylines, npj Climate and Atmospheric Science, 7, 1–14, https://doi.org/10.1038/s41612-024-00759-2, 2024.

Merrifield, A., Lehner, F., Xie, S.-P., and Deser, C.: Removing Circulation Effects to Assess Central U.S. Land-Atmosphere Interactions in the CESM Large Ensemble, Geophysical Research Letters, 44, 9938–9946, https://doi.org/10.1002/2017GL074831, 2017.

Merrifield, A., Lehner, F., Lorenz, R., and Knutti, R.: Exploring Extended Warm Periods in an Observational Large Ensemble of Historical European Temperature, in: AGU Fall Meeting Abstracts, vol. 2020, pp. GC058–0005, 2020.

Pfleiderer, P., Schleussner, C.-f., Kornhuber, K., and Coumou, D.: Summer Weather Becomes More Persistent in a 2 °C World, Nature Climate Change, https://doi.org/10.1038/s41558-019-0555-0, 2019.

Qasmi, S. and Ribes, A.: Reducing Uncertainty in Local Temperature Projections, Science Advances, 8, eabo6872, https://doi.org/10.1126/sciadv.abo6872, 2022.

Rayner, N. A., Parker, D. E., Horton, E. B., Folland, C. K., Alexander, L. V., Rowell, D. P., Kent, E. C., and Kaplan, A.: Global Analyses of Sea Surface Temperature, Sea Ice, and Night Marine Air Temperature since the Late Nineteenth Century, Journal of Geophysical Research: Atmospheres, 108, https://doi.org/10.1029/2002JD002670, 2003.

Rigal, A., Azaïs, J.-M., and Ribes, A.: Estimating Daily Climatological Normals in a Changing Climate, Climate Dynamics, 53, 275–286, https://doi.org/10.1007/s00382-018-4584-6, 2019.

Rodgers, K. B., Lee, S.-S., Rosenbloom, N., Timmermann, A., Danabasoglu, G., Deser, C., Edwards, J., Kim, J.-E., Simpson, I. R., Stein, K., Stuecker, M. F., Yamaguchi, R., Bódai, T., Chung, E.-S., Huang, L., Kim, W. M., Lamarque, J.-F., Lombardozzi, D. L., Wieder, W. R., and Yeager, S. G.: Ubiquity of Human-Induced Changes in Climate Variability, Earth System Dynamics, 12, 1393–1411, https://doi.org/10.5194/esd-12-1393-2021, 2021.

Ronneberger, O., Fischer, P., and Brox, T.: U-Net: Convolutional Networks for Biomedical Image Segmentation, 2015.

Röthlisberger, M. and Papritz, L.: Quantifying the Physical Processes Leading to Atmospheric Hot Extremes at a Global Scale, Nature Geoscience, 16, 210–216, https://doi.org/10.1038/s41561-023-01126-1, 2023.

https://doi.org/10.5194/egusphere-2025-2397
Preprint. Discussion started: 4 June 2025

Rousi, E., Kornhuber, K., Beobide-Arsuaga, G., Luo, F., and Coumou, D.: Accelerated Western European Heatwave Trends Linked to More-Persistent Double Jets over Eurasia, Nature Communications, 13, 3851, https://doi.org/10.1038/s41467-022-31432-y, 2022.

Saffioti, C., Fischer, E. M., and Knutti, R.: Improved Consistency of Climate Projections over Europe after Accounting for Atmospheric Circulation Variability, Journal of Climate, 30, 7271–7291, https://doi.org/10.1175/JCLI-D-16-0695.1, 2017.

Seneviratne, S. I., Lüthi, D., Litschi, M., and Schär, C.: Land–Atmosphere Coupling and Climate Change in Europe, Nature, 443, 205–209, https://doi.org/10.1038/nature05095, 2006.

Seneviratne, S. I., Zhang, X., Adnan, M., Badi, W., Dereczynski, C., Di Luca, A., Vicente-Serrano, S. M., Wehner, M., and Zhou, B.: Chapter 11: Weather and Climate Extreme Events in a Changing Climate. In Climate Change 2021: The Physical Science Basis., 2021.

Shaw, T. A. and Miyawaki, O.: Fast Upper-Level Jet Stream Winds Get Faster under Climate Change, Nature Climate Change, 14, 61–67, https://doi.org/10.1038/s41558-023-01884-1, 2024.

Shepherd, T. G.: Atmospheric Circulation as a Source of Uncertainty in Climate Change Projections, Nature Geoscience, 7, 703–708, https://doi.org/10.1038/ngeo2253, 2014.

Shepherd, T. G.: Storyline Approach to the Construction of Regional Climate Change Information, Proceedings of the Royal Society A: Mathematical, Physical and Engineering Sciences, 475, https://doi.org/10.1098/rspa.2019.0013, 2019.

Singh, J., Sippel, S., and Fischer, E. M.: Circulation Dampened Heat Extremes Intensification over the Midwest USA and Amplified over Western Europe, Communications Earth & Environment, 4, 1–9, https://doi.org/10.1038/s43247-023-01096-7, 2023.

Sippel, S., Meinshausen, N., Merrifield, A., Lehner, F., Pendergrass, A. G., Fischer, E., and Knutti, R.: Uncovering the Forced Climate Response from a Single Ensemble Member Using Statistical Learning, Journal of Climate, 32, 5677–5699, https://doi.org/10.1175/JCLI-D-18-0882.1, 2019.

Sippel, S., Barnes, C., Cadiou, C., Fischer, E., Kew, S., Kretschmer, M., Philip, S., Shepherd, T. G., Singh, J., Vautard, R., and Yiou, P.: Could an Extremely Cold Central European Winter Such as 1963 Happen Again despite Climate Change?, Weather and Climate Dynamics, 5, 943–957, https://doi.org/10.5194/wcd-5-943-2024, 2024.

Smoliak, B. V., Wallace, J. M., Lin, P., and Fu, Q.: Dynamical Adjustment of the Northern Hemisphere Surface Air Temperature Field: Methodology and Application to Observations, Journal of Climate, 28, 1613–1629, https://doi.org/10.1175/JCLI-D-14-00111.1, 2015.

Teng, H., Leung, R., Branstator, G., Lu, J., and Ding, Q.: Warming Pattern over the Northern Hemisphere Midlatitudes in Boreal Summer 1979–2020, Journal of Climate, 35, 3479–3494, https://doi.org/10.1175/JCLI-D-21-0437.1, 2022.

Terray, L.: A Dynamical Adjustment Perspective on Extreme Event Attribution, Weather and Climate Dynamics, 2, 971–989, https://doi.org/10.5194/wcd-2-971-2021, 2021.

Topál, D. and Ding, Q.: Atmospheric Circulation-Constrained Model Sensitivity Recalibrates Arctic Climate Projections, Nature Climate Change, 13, 710–718, https://doi.org/10.1038/s41558-023-01698-1, 2023.

Van Den Dool, H. M.: Searching for Analogues, How Long Must We Wait?, Tellus A, 46, 314–324, https://doi.org/10.1034/j.1600-0870.1994.t01-2-00006.x, 1994.

Vautard, R., Cattiaux, J., Happé, T., Singh, J., Bonnet, R., Cassou, C., Coumou, D., D'Andrea, F., Faranda, D., Fischer, E., Ribes, A., Sippel, S., and Yiou, P.: Heat Extremes in Western Europe Increasing Faster than Simulated Due to Atmospheric Circulation Trends, Nature Communications, 14, 6803, https://doi.org/10.1038/s41467-023-42143-3, 2023.

Wehrli, K., Guillod, B. P., Hauser, M., Leclair, M., and Seneviratne, S. I.: Assessing the Dynamic Versus Thermodynamic Origin of Climate Model Biases, Geophysical Research Letters, 45, 8471–8479, https://doi.org/10.1029/2018GL079220, 2018.

https://doi.org/10.5194/egusphere-2025-2397
Preprint. Discussion started: 4 June 2025

Wills, R. C. J., Battisti, D. S., Armour, K. C., Schneider, T., and Deser, C.: Pattern Recognition Methods to Separate Forced Responses from Internal Variability in Climate Model Ensembles and Observations, Journal of Climate, 33, 8693–8719, https://doi.org/10.1175/JCLI-D-19-0855.1, 2020.

Woollings, T., Drouard, M., O'Reilly, C. H., Sexton, D. M. H., and McSweeney, C.: Trends in the Atmospheric Jet Streams Are Emerging in Observations and Could Be Linked to Tropical Warming, Communications Earth & Environment, 4, 1–8, https://doi.org/10.1038/s43247-023-00792-8, 2023.

Zeder, J. and Fischer, E. M.: Quantifying the Statistical Dependence of Mid-Latitude Heatwave Intensity and Likelihood on Prevalent Physical Drivers and Climate Change, Advances in Statistical Climatology, Meteorology and Oceanography, 9, 83–102, https://doi.org/10.5194/ascmo-9-83-2023, 2023.